Acta Manilana 68 (2020), 1–11

ISSN: 0065–1370

Acta Manilana

journal homepage: journals.ust.edu.ph

Colorimetric detection of cadmium(II) using glutathione-capped gold nanoparticles

Alan Rodelle M. Salcedo*, Nova Carisa F. Morabe, & Fortunato B. Sevilla III

Department of Chemistry, College of Science; Research Center for Natural and Applied Sciences, University of Santo Tomas, España Boulevard, 1015 Manila, The Philippines

Graphical Abstract

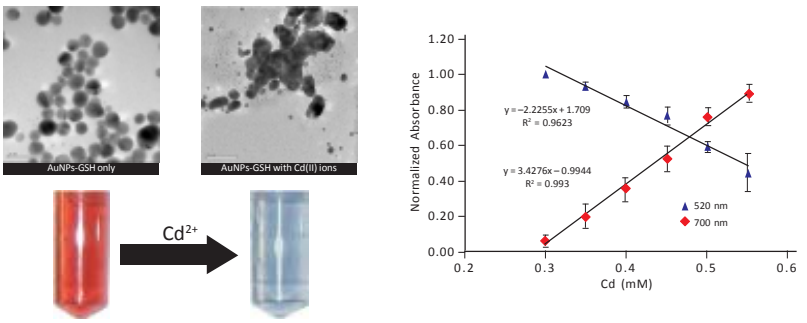

Abstract

Glutathione-capped gold nanoparticles (GSH-AuNPs) were prepared by chemical reduction of $HAuCl_4$ using glutathione (GSH) as the capping agent and $NaBH_4$ as the reducing agent. GSH-AuNPs were characterized by UV-Vis spectroscopy, IR spectroscopy, and transmission electron microscopy (TEM). The pH value of the synthesized GSH-AuNPs solution was also measured to be 7.20. A colorimetric method for Cd^{2+} was developed based on the aggregation of GSH-AuNPs induced by its interaction with Cd^{2+}, which is also exhibited as a red to blue color change. At pH 6, the GSH-AuNPs-based colorimetric method exhibited higher sensitivity and better linearity at 700 nm. Stable absorbance readings were established at 10 min reaction time. Under the optimized conditions, this method was found to be linear (linearity of 0.993 r^2) in the concentration range of 0.3–0.55 mM with sensitivity of 3.43 A.U./mM and detection limit of 1.35×10^{-3} mM. With its good analytical performance such as low cost, sensitivity, rapidity, and visual detection, the GSH-AuNPs-based method described here demonstrates potential application for the detection of Cd^{2+} in actual water sample for assessment and monitoring purpose.

Keywords: colorimetric sensor, gold nanoparticles, glutathione, cadmium

Corresponding author at: Research Center for the Natural and Applied Sciences, University of Santo Tomas, Manila, The Philippines
Email address: *amsalcedo@ust.edu.ph*

Introduction

Cadmium ions (Cd^{2+}), like many other heavy transition metals, are toxic to living cells and cause a serious threat to human health and environment. It is listed by the US Environmental Protection Agency as one of 126 priority pollutants [1]. It has also been linked to various toxic effects on kidneys, liver, lungs, bones, cardiovascular, endocrine, reproductive system, as well several diseases such as osteoporosis, hypertension, non-hypertrophic emphysema, irreversible renal tubular injury, anemia, eosinophilia, anosmia, and chronic rhinitis [2–5]. The risks of cadmium to environmentally exposed populations were highlighted, when it was shown to be the main cause of the infamous Itai-itai disease (Japanese for Ouch-Ouch disease), a bone disease with fractures and severe pain.

Cadmium is one of the heavy metals that occur in acidic drainage from sites where metals such as silver, gold, copper, and zinc are mined. This drainage spills into the rivers and eventually to the sea, causing damage to aquatic life. A very high level of cadmium (811–846 mg/L) has been noted in the creeks near the Lafayette mine in Rapu Rapu Island, Albay where massive fish kills occurred in October 2005 [6]. This concentration is several hundred times higher than 5 mg/L which has been shown to produce harmful effects to many aquatic species [7]. Cadmium is also generated in some electroplating processes and in metal recovery operations in the recycling of electronics. It is one of the toxic contaminants in the wastewater produced by industries involving these processes and released into the adjacent rivers. Excess levels of Cd^{2+} have been found by the Environmental Management Bureau (EMB) in Marilao River, Bocaue River and Meycauyan River in Bulacan where electroplating and metal recycling plants are found along the banks of these rivers [8, 9].

Currently, a number of analytical techniques have been applied to determine Cd^{2+} in different biological and environmental samples including atomic absorption spectrometry (AAS) [10, 11], quartz crystal microbalance [12, 13], and electrochemical sensing [14–17]. AAS-based methods are sensitive and rapid but commonly suffer from interferences due to particles and nonspecific absorption that causes light scattering [18]. Electrochemical sensing using electroanalytical principles such as polarography, potentiometry, and voltammetry offers advantages such as specific sensitivity, faster response time, low detection limit, and good selectivity. In the work of Arabi and co-workers [14], an electrochemical sensor for Cd^{2+} in water samples using clay/carbon nanocomposite modified with an organic ligand exhibited a good selectivity for Cd(II) in the range of 2.0–100.0 ppb and a detection limit of 0.7 ppb. Conventional colorimetric methods for Cd have been primarily based on dithizone as reagent. Methods using this reagent present a low detection limit but suffer from poor specificity. And to improve the method's selectivity, additional extraction-separation step must first be carried out.

Gold nanoparticle (AuNP) is one of the most studied nanomaterials because of their novel properties arising from its nanometer size dimension. Its use in chemical sensors, biosensors and other sensing systems are due to its optical properties and are attributed to the localized surface plasmon resonance (LSPR) originating from the

excitation of the free electrons collectively oscillating in the conduction band on the surface of the nanoparticles. The adsorption maximum, intensity, and width of the LSPR band are particularly dependent on size, shape, composition, and local dielectric environment of the nanoparticles making it possible to be utilized for sensing applications [19].

AuNPs-based colorimetric sensors have been widely explored and have been applied for the sensitive detection of different analytes such as heavy metal ions [20], peptide and protein [21, 22], and DNA [23]. Detection of such analytes is primarily based on monitoring the shifts, complete disappearance (and/or simultaneous appearance of another band), or change in the structure or intensity in LSPR absorption band. The LSPR property of AuNPs can also facilitate naked-eye detection on the basis of nanoparticles aggregation without sacrificing the selectivity and sensitivity of the detection scheme. In the study of Boruah and Biswas [24], polyethylene glycol (PEG)-functionalized AuNPs was utilized as colorimetric reagent for arsenic in aqueous medium. The detection was established by the selective interaction of the negative surface of PEG-functionalized AuNPs with As^{3+}, which resulted to the red to blue color change in the solution as a result of the AuNP aggregation. With valine-capped AuNPs, free $–COO^-$ groups on the AuNPs surface interacted with Pb^{2+} leading to the cross-linking of particles and consequent aggregation. This selective interaction of valine-capped AuNPs lead to the selective detection of Pb^{2+} in the range of 0–100 ppm with detection limit of 30.5 μM [25].

In the past years, a number of studies have reported different colorimetric sensing methods employing GSH-AuNPs for detection of metal ions such as calcium (Ca^{2+}) [26], nickel (Ni^{2+}) [27], and lead (Pb^{2+}) [28–31] where the later has been mostly the analyte of interest because of the stronger affinity between Pb^{2+} and -COOH in GSH than that of other heavy metal ions. In a study of Feng and co-workers [28], the sensor fabricated from GSH-AuNPs self-assembled on a transparent indium tin oxide exhibited red-shift that is linearly proportional to Pb^{2+} concentration from 10^{-10} to 10^{-5} M and a detection limit of 5×10^{-11} M. The strong affinity of Pb^{2+} with GSH caused the red shift of the LSPR peak.

In this study, we report a GSH-AuNP-based colorimetric method for Cd^{2+}. The proposed colorimetric method is based from experimental observation that GSH-AuNPs solution exhibits a red-to-blue color change upon addition of Cd^{2+} solutions. The limit of detection (LOD) for this method is 1.35×10^{-3} mM. This method offers a cheap, simple and rapid detection scheme for Cd^{2+} in aqueous media.

Materials and methods

Materials. All chemicals used were of analytical reagent grade (AR) and were used as received without further purification. Hydrogen tetrachloroaurate ($HAuCl_4 \cdot 3H_2O$ ≥ 99%), L-glutathione reduced (≥99%), sodium borohydride (98+%), $CaCl_2 \cdot H_2O$ (≥99%), $CdN_2O_6 \cdot H_2O$ (99.999%), $Co(CH_3COO) \cdot 4H_2O$, $CrN_3O_9 \cdot 9H_2O$ (99%), $Pb(NO_3)_2$ (99.999% metal basis), $MgN_2O_6 \cdot H_2O$, $Zn(CH_3COO)_2 \cdot 2H_2O$ (99.99%), $Ni(NO_3)_2 \cdot 6H_2O$ (99.999%), $Mn(NO_3)_2 \cdot xH_2O$, $CuSO_4 \cdot 5H_2O$, and $FeCl_3 \cdot 6H_2O$ were purchased from Sigma-Aldrich.

All glassware were cleaned with freshly prepared 3:1 HCl/HNO_3 (aqua regia), rinsed thoroughly with ultrapure water and oven-dried prior to use. All solutions were prepared using ultrapure water (TOC <5.00 pbb; resistivity: 18.2 $M\Omega cm^{-1}$).

Synthesis of glutathione-capped gold nanoparticles (GSH-AuNPs). GSH-AuNPs were prepared by chemical reduction method. In a typical synthesis, 50 mL of 1.0 mM of tetrachloroauric acid ($HAuCl_4 \cdot 3H_2O$) was mixed with 50 mL of 0.25 μM aqueous GSH solution. The mixture was stirred for 30 min prior to the addition of freshly prepared $NaBH_4$ (200 μL, 1.0 M). Then, the resulting solution was stirred for another 30 min to allow the completion of reaction. The solution was then cooled to room temperature and stored overnight prior measurement of initial pH and further characterization. The red colored solution is evident of the formation of AuNPs.

Characterization of GSH-AuNPs

Spectroscopic measurements. The UV-Vis absorption spectra were obtained at room temperature (~30°C ± 2) using Perkin Elmer Lambda 35 spectrometer equipped with UVWINLAB v.2.85 software employing 1 cm quartz cuvettes as sample holder. Fourier transform infrared (FT-IR) spectroscopy was performed on a Perkin Elmer Spectrum Two™ spectrometer with a universal attenuated total reflectance (UATR) attachment operating between 400 and 4000 cm^{-1}. Prior to IR measurements, GSH-AuNPs powder was obtained by centrifugation at 14,000 rpm (4°C) for 15 min and stored in a desiccator overnight to removed excess water from the powder. The dried GSH-AuNPs powder was pressed on the diamond crystal of the ATR attachment. Infrared spectra were then recorded with 4 cm^{-1} resolution.

Transmission electron microscopy (TEM) . Samples were prepared for TEM analysis by drop-casting ~5 mL on Formvar-coated copper grids and were dried inside a desiccator for a few minutes. The TEM analysis was performed using Philips Tecnai G2 20 S-TWIN with an accelerating voltage of 200 kV. The TEM micrographs obtained were then analyzed using ImageJ 1.44p software for particle diameter measurements.

Colorimetric assay of Cd^{2+}. GSH-AuNPs solution were mixed with aqueous Cd^{2+} solutions in a 1:1 v/v ratio. The initial concentrations of Cd^{2+} used were 0.1 mM, 0.2 mM, 0.3 mM, 0.35 mM, 0.4 mM, 0.45 mM, 0.5 mM, 0.55 mM, 0.6 mM, and 0.7 mM. Suitable blank solutions (without GSH-AuNPs solutions) were also prepared. Any pH value adjustments of the GSH-AuNPs solutions prior to UV-Vis measurements were made using 0.10 M HCl.

The effect of reaction time was investigated using the time drive method of the UVWINLAB v.2.85 software. Working wavelength was selected by comparing the calibration curves obtained from 520 nm and 700 nm. Normalized absorbance readings were used to construct all calibration curves studied.

The interference was carried out using 0.10 and 0.010 mM aqueous solutions of the following ions: Ca^{2+}, Co^{2+}, Cr^{3+}, Cu^{2+}, Fe^{3+}, Mg^{2+}, Mn^{2+}, Ni^{2+}, Pb^{2+}, and Zn^{2+}. Effect of these ions on GSH-AuNPs was investigated at 700 nm.

Results and discussion

Synthesis and characterization of GSH-AuNPs. Glutathione, a tripeptide of glutamate, cysteine, and glycine, is generally known as an antioxidant. It contains functional groups, including amino, carboxylic and thiol group, which are potential active sites for surface modification of nanoparticles and chelation of metal ions. In the synthesis of AuNPs, GSH was used as the capping agent with $NaBH_4$ as the reducing agent. The formation of GSH-AuNPs using this method follows the mechanism proposed in the work of Briñas and co-workers [32]. In the described mechanism, Au^{3+} is first reduced by the GSH molecule to Au^{1+}. Then, a polymeric structure of Au^{1+} ($[Au(I)SG]_n$) is formed where the thiolate sulfur atom of GSH is linked to Au^{1+}. This polymeric structure is then decomposed to AuNPs through the addition of $NaBH_4$. The UV-Vis spectrum of the synthesized GSH-AuNPs exhibits an LSPR absorption band of 520 nm (Fig. 1a). The average particle diameter of the GSH-AuNPs is 5.67 nm. TEM micrograph and histogram of the particle diameter distribution is shown in Fig. 1b and 1c.

For the infrared spectroscopic characterization of the synthesized GSH-AuNPs, comparison of the IR spectrum of the GSH-AuNPs with the free GSH showed that the absorption peak at 2523 cm^{-1} corresponding to the presence of thiol group (-SH) in the free GSH disappeared in the IR spectrum of the synthesized GSH-AuNPs (Fig. 2). This observation confirms that the conjugation of the GSH molecules to the AuNPs is through the S to Au thiolate linkage. However, characteristic absorption bands pertaining to the N-H stretch in the free GSH (~3375 cm^{-1} and ~3250 cm^{-1}) were observed to shift to 3187 cm^{-1} and became broader. This suggests that GSH molecules can also bind to AuNPs through the nitrogen atom. Another observation was the disappearance of the sharp absorption band at 1710 cm^{-1} which is attributed to the carbonyl (C=O) stretching vibration of the carboxylic acid group of the free GSH.

Effect of pH and Cd^{2+} on GSH-AuNPs. The AuNPs are stably dispersed due to the GSH functionalization attached to its surface. The stability provided by the GSH

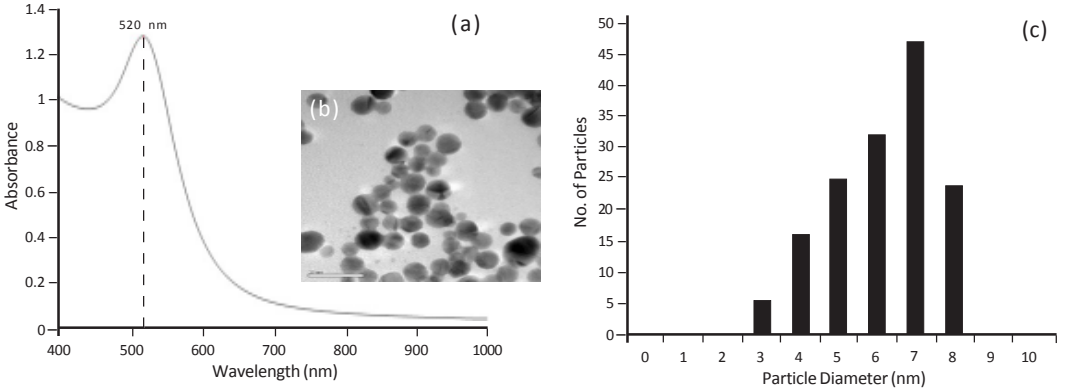

Figure 1. (a) UV-Vis absorption spectrum, (b) TEM micrograph, and (c) particle diameter distribution of the synthesized GSH-AuNPs

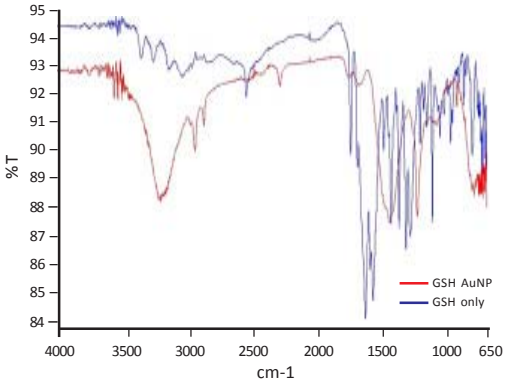

Figure 2. Infrared spectra of free GSH and GSH-AuNPs

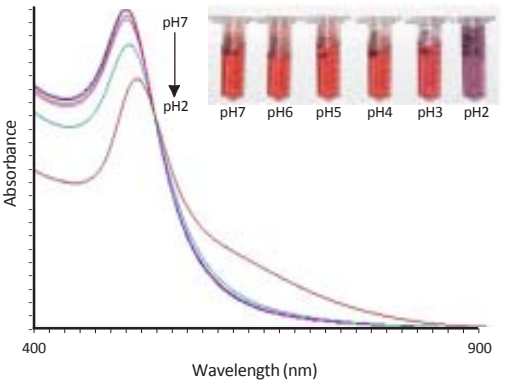

Figure 4. Image and UV-Vis spectra of GSH-AuNPs adjusted to different pH values

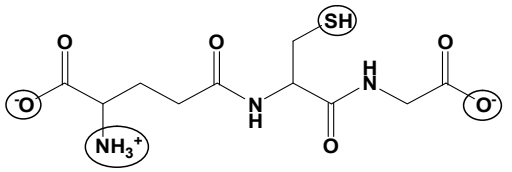

Figure 3. Glutathione molecule at pH 7 with its four ionizable functional groups.

molecule can be due to the repulsive electrostatic forces among the GSH molecules. Since GSH has four ionizable functional groups, the amino (-NH_2), the two carboxylic (-COOH) and the thiol (-SH) groups, the strength of the repulsion forces among them can be dependent on its pH. Since the synthesized GSH-AuNPs has a measured pH value of 7.20, most GSH molecules at this pH has a –1 net charge [33] (Fig. 3). This, therefore, provides negative charge to the surface of the AuNPs, thus having enough repulsion forces among the GSH-AuNPs.

Upon addition of 0.10 M HCl to the GSH-AuNPs solution, its color changed from red to violet only when the pH value reached 2. At this point the AuNPs has already aggregated. The GSH-AuNPs from pH 6 to pH 3 still exhibits a red coloration indicating its dispersion and stability. As seen in the UV-Vis spectra, very minimal changes are noticed from pH values 6 to 4. At pH 3, there was already a noticeable lowering in the absorbance and at pH 2, lowering of the absorbance coupled with the red shifting of the LSPR absorption band was already observed. The appearance of a shoulder peak is also very evident which an indication that the AuNPs have aggregated at this pH value. These observations suggest that the AuNPs are still stable at pH value 6 to 4, but already unstable at pH value 2.

In the analyses to investigate the effect of Cd^{2+}, it was observed that the GSH-AuNPs solutions immediately changed from red to purple with the 10^{-4} M Cd^{2+} and changed from red to blue with 10^{-3} M, 10^{-2} M and 10^{-1} M Cd^{2+}. This Cd^{2+}-induced aggregation of GSH-AuNPs can be due to the formation of Cd^{2+} complexes with the GSH molecules bound to the surface of the AuNPs. Although the binding of Cd^{2+} to GSH is complicated because the four active site in GSH may undergo protonation or deprotonation and because different stoichiometries could form in its complexes [33], in can still be assumed that the Cd^{2+} binds with the two deprotonated carboxyl

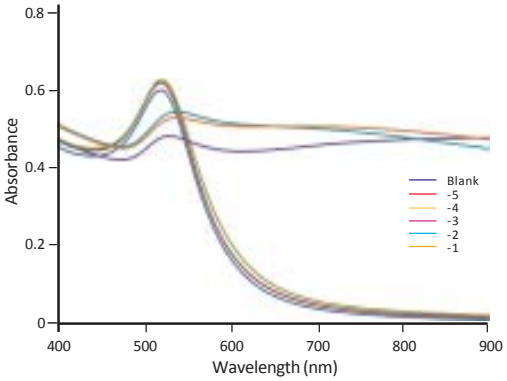

Figure 5. UV-Vis absorption spectra of GSH-AuNPs with different Cd(II) ion concentrations

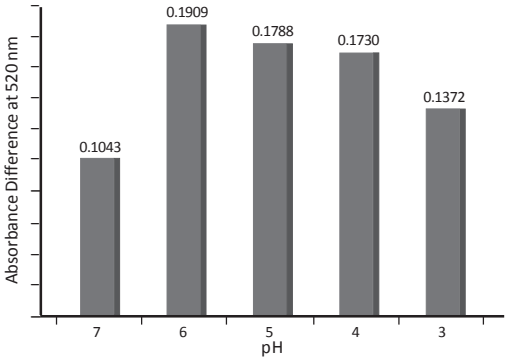

Figure 6. Summary of absorbance difference of GSH-AuNPs for 10^{-1} M and 10^{-5} M Cd^{2+}

groups ($–COO^-$) of the GSH molecule. With 10^{-5} M Cd^{2+}, no aggregation was observed since the color of the GSH-AuNPs solution remained unchanged.

The aggregation of GSH-AuNPs can also be observed in the UV-Vis absorption spectra (Fig. 5). With the addition of Cd^{2+}, shifts in the LSPR absorption bands to the longer wavelength were observed. These red shifts were very evident for Cd^{2+} concentration of 10^{-3} M, 10^{-2} M, and 10^{-1} M and were coupled with decrease in the absorption intensities at 520 nm and increase in the absorption intensities at the longer wavelengths. For 10^{-5} M and 10^{-4} M, changes observed were very minimal.

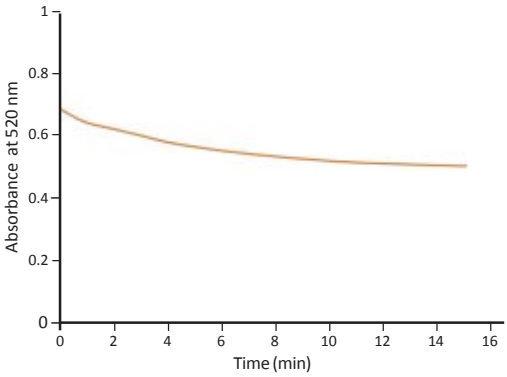

Figure 7. Time-dependent absorbance at 520 nm of GSH-AuNPs after addition of 10^{-4} M Cd

The Cd(II) ions-induced aggregation of GSH-AuNPs was also noticed to be affected by the pH value of the solution. By adjusting the pH values of the GSH-AuNPs solutions prior to addition of 10^{-5} M and 10^{-1} M of Cd^{2+}, more prominent and faster color change were noticed at lower pH values. To further evaluate its effect, the absorbance differences at 520 nm for the two concentrations were plotted at different pH values. As seen in Fig. 6, highest absorbance difference is exhibited at pH value 6. Since the absorbance at 520 nm represents the amount of dispersed or unaggregated AuNPs, a decrease in its intensity suggests that the nanoparticles have aggregated. The magnitude of decrease in its intensity also represents the extent of aggregation caused by the Cd^{2+}. Since the highest absorbance difference was observed at pH 6, highest sensitivity of GSH-AuNPs for Cd^{2+} will therefore be achieved at this pH value.

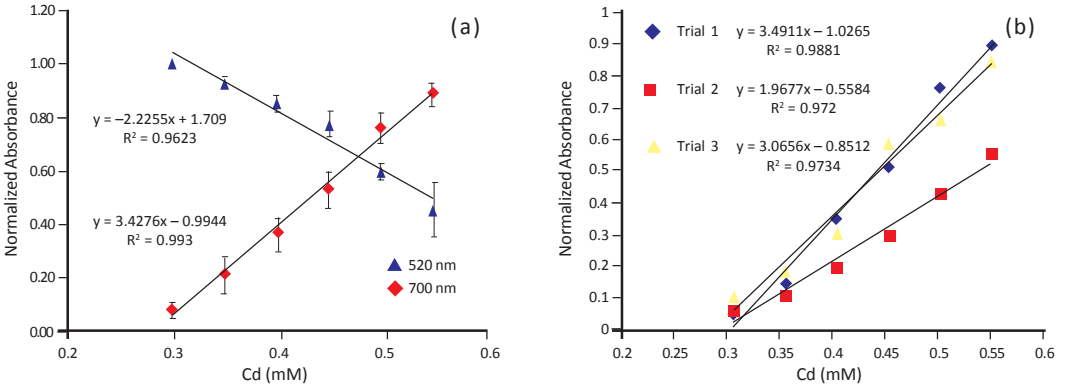

Figure 8. (a) Comparison of linear curve obtained from 520 nm and 700 nm and (b) Calibration curve for Cd(II) ions obtained from three different days.

Colorimetric assay of* Cd^{2+} *using GSH-AuNPs. Cd^{2+} can be quantitated based on its aggregation effects on GSH-AuNPs. The aggregation can be monitored visually through the color change in the solution and spectrophotometrically through careful analysis of the change in the absorption spectra. Since the color change in GSH-AuNPs solution is based on the formation of aggregates, the time dependence of its formation was also investigated to study its extent and stability. For this experiment, 10^{-4} M Cd^{2+} was used to react with the GSH-AuNPs. After about 10 min, the absorbance changes at 520 nm are very minimal. This observation suggests that the aggregates formed are already stable. At this point, good reproducibility was attained for the absorbance readings.

Initial assessments have shown that the change in color of the GSH-AuNPs solution is also dependent on the concentration of Cd^{2+}. The dynamic working range was established from the plot of the normalized absorbance values at 520 nm against the –log of Cd^{2+} concentrations. Based on this plot, a linear behavior was established within the Cd^{2+} concentration range of 0.30–0.55 mM. In an attempt to further improved the characteristics of the linear curve (i.e. linearity and sensitivity), we compared the linear curve obtained from normalized absorbance value at 520 nm and 700 nm. As seen in Fig. 8a, the linear curve for the same concentration range obtained from 700 nm has better linearity and sensitivity than the curve obtained from 520 nm. For the calibration curve obtained from 700 nm, the detection limit that is taken to be three times the standard derivation in blank solution was calculated to be 1.35×10^{-3} mM. The reproducibility of the colorimetric assay was also evaluated by comparing the calibration curves obtained at the optimized conditions in three different days. It can be seen from Figure 8b that the linearity and sensitivity of the calibration curves obtained in three different days are very comparable except only for the sensitivity obtained from trial 2.

In the analyses of metal ion interferences, it was found out that the ions Cr^{3+}, Fe^{3+}, and Pb^{2+} also caused the GSH-AuNPs to aggregate when they are at least at 0.1 mM concentration. Among these three interferences, Pb^{2+} was identified as the highest

interfering ion. Although it was initially thought that affinity of Cd^{2+} to thiol group is stronger than Pb^{2+} based from the HSAB concept [34], this behavior could have arise from the stronger affinity of Pb^{2+} to the carboxyl (-COOH) groups [35] of the GSH. At 0.010 mM and 0.0010 mM metal ion concentrations, no interfering ion was identified.

Conclusion

In conclusion, GSH-AuNPs were successfully synthesized by reduction of $HAuCl_4$ in the presence of GSH using $NaBH_4$. Aggregation of the GSH-AuNPs was demonstrated to be dependent on factors such as variation in the pH and presence of Cd^{2+} ions. The GSH attached to the surface of the AuNPs provides reactivity towards complexation of metal ions due to –COOH, $–NH_2$ and –SH groups. The aggregation behavior of GSH-AuNPs in the presence of Cd(II) ions leads to the visible color change from red to violet coupled with shifts in the absorption spectrum leading to a simple, inexpensive and rapid colorimetric assay for metal ion such as Cd(II). The method described herein showed considerable linearity and sensitivity towards Cd(II) ions with the limit of detection of 0.00135 mM. Since the interfering ions, Cr^{3+}, Fe^{3+}, and Pb^{2+}, were identified, efforts to improve the selectivity of the assay is in progress. The GSH-AuNPs-based colorimetric assay described here demonstrates potential application for the assessment and monitoring of water quality.

Acknowledgment

This work was financially supported by the National Philippine Council for Industry, Energy, and Emerging Technology Research and Development (PCIEERD).

References

[1] Waisberg M, Joseph P, Hale B, & Beyersmann D. Molecular and cellular mechanisms of cadmium carcinogenesis. *Toxicology* **2003**; 192(2–3), 95–117. DOI: 10.1016/S0300-483X(03)00305-6

[2] Tchounwou PB, Yedjou CG, Patlolla AK, & Sutton DJ. Heavy Metal Toxicity and the Environment. In: Luch A (Ed.) *Molecular, Clinical and Environmental Toxicology (Volume 3: Environmental Toxicology). Experientia Supplementum* (Vol. 101), pp. 133-164). (Germany: Springer Basel AG, **2012**). DOI: 10.1007/978-3-7643-8340-4_6

[3] Joseph P. Mechanisms of cadmium carcinogenesis. *Toxicology and Applied Pharmacology* **2009**; 238(SI3), 272–279. DOI: 10.1016/j.taap.2009.01.011

[4] Nordberg GF. Historical perspectives on cadmium toxicology. *Toxicology and Applied Pharmacology* **2009**; 238(SI3), 192–200. DOI: 10.1016/j.taap.2009.03.015

[5] Waalkes MP. Cadmium carcinogenesis in review. *Journal of Inorganic Biochemistry* **2000**; 79(1–4), 241–244. DOI: 10.1016/S0162-0134(00)00009-X

[6] Brigden K & Cotter J. Pollution from the Lafayette mine, Rapu Rapu (Philippines) during 30-day trial run *Greenpeace Research Laboratories Technical Note 10/2006* **2006 October**.

[7] Bryan GW & Langston WJ. Bioavailability, accumulation and effects of heavy metals in sediments with special reference to United Kingdom estuaries: a review. *Environmental Pollution* **1992**; 76(2), 89–131. DOI: 10.1016/0269-7491(92)90099-V

[8] Greenpeace. *Climate Change and Water: Impacts and Vulnerabilities in the Philippines*. (Philippines: Greenpeace Southeast Asia, **2009**).

[9] Greenpeace. *The state of water resources in the Philippines*. (Philippines: Greenpeace Southeast Asia, **2007**).

[10] Golbedaghi R, Jafari S, Yaftian MR, Azadbakht R, Salehzadeh S, & Jaleh B, Determination of cadmium(II) ion by atomic absorption spectrometry after cloud point extraction. *Journal of the Iranian Chemical Society* **2012**; 9(3), 251–256. DOI: 10.1007/s13738-011-0018-7

[11] Payehghadr M, Esmaeilpour S, Kazem Rofouei M, & Adlnasab L. Determination of trace amount of cadmium by atomic absorption spectrometry in table salt after solid phase preconcentration using octadecyl silica membrane disk modified by a new derivative of pyridine. *Journal of Chemistry* **2013**; 2013, Art. No. 417085. DOI: 10.1155/2013/417085

[12] Taneja P, Manjuladevi V, Gupta R, & Gupta RK. Detection of Cadmium Ion in Potable Water Using Quartz Crystal Microbalance. *Macromolecular Symposia* **2017**; 376(1), Art. No. 1600207. DOI: 10.1002/masy.201600207

[13] Taneja P, Manjuladevi V, Gupta KK, & Gupta RK. Detection of cadmium ion in aqueous medium by simultaneous measurement of piezoelectric and electrochemical responses. *Sensors and Actuators B: Chemical* **2018**; 268, 144–149. DOI: 10.1016/j.snb.2018.04.091

[14] Sheikh Arabi M, Karami C, & Ghanei-Motlagh M. Fabrication of a Novel Electrochemical Sensor for Simultaneous Determination of Toxic Lead and Cadmium Ions. *Annals of Military and Health Sciences Research* **2019**; 17(4). Art. No. e99082. DOI: 10.5812/amh.99082

[15] Ourari A, Tennah F, Ruíz-Rosas R, Aggoun D, & Morallón E. Bentonite modified carbon paste electrode as a selective electrochemical sensor for the detection of Cadmium and Lead in aqueous solution. *International Journal of Electrochemical Science* **2018**; 13(2), 1683–1699. DOI: 10.20964/2018.02.35

[16] Rezvani Ivari SA, Darroudi A, Arbab Zavar MH, Zohuri G, & Ashraf N. Ion imprinted polymer based potentiometric sensor for the trace determination of Cadmium (II) ions. *Arabian Journal of Chemistry* **2017**; 10(S1), S864–S869. DOI: 10.1016/j.arabjc.2012.12.021

[17] Aglan RF, Hamed MM, & Saleh HM. Selective and sensitive determination of Cd(II) ions in various samples using a novel modified carbon paste electrode. *Journal of Analytical Science and Technology* **2019**; 10, Art. No. 7. DOI: 10.1186/s40543-019-0166-4

[18] *International Programme on Chemical Safety (IPCS)* Environmental Health Criteria 134: Cadmium, 84 (n.d.). www.inchem.org/documents/ehc/ehc/ehc134.htm (2019 May 7)

[19] Khan I, Saeed K, & Khan I. Nanoparticles: Properties, applications and toxicities. *Arabian Journal of Chemistry* **2019**; 12(7), 908–931. DOI: 10.1016/j.arabjc.2017.05.011

[20] Sener G, Uzun L, & Denizli A. Colorimetric sensor array based on gold nanoparticles and amino acids for identification of toxic metal ions in water. *ACS Applied Materials and Interfaces* **2014**; 6(21), 18395–18400. DOI: 10.1021/am5071283

[21] Retout M, Valkenier H, Triffaux E, Doneux T, BartikK, & Bruylants G. Rapid and Selective Detection of Proteins by Dual Trapping Using Gold Nanoparticles Functionalized with Peptide Aptamers. *ACS Sensors* **2016**; 1(7), 929–933. DOI: 10.1021/acssensors.6b00229

[22] Chang K, Wang S, Zhang H, Guo Q, Hu X, Lin Z, Sun H, Jiang M, & Hu J. Colorimetric detection of melamine in milk by using gold nanoparticles-based LSPR via optical fibers' *PLoS One.* **2017**; 12(5), Art. No. e0177131. DOI: 10.1371/journal.pone.0177131

[23] Aliofkhazraei M (Ed.). *Handbook of Nanoparticles* **2016**. DOI: 10.1007/978-3-319-15338-4

[24] Boruah BS & Biswas R. Selective detection of arsenic (III) based on colorimetric approach in aqueous medium using functionalized gold nanoparticles unit. *Materials Research Express* **2018**; 5(1), Art. No. 015059. DOI: 10.1088/2053-1591/aaa661

[25] Priyadarshini E & Pradhan N. Metal-induced aggregation of valine capped gold nanoparticles: An efficient and rapid approach for colorimetric detection of Pb2+ ions. *Scientific Reports* **2017**; 7, Art. No. 9278. DOI: 10.1038/s41598-017-08847-5

[26] Gong W, Bai L, Cui C, Zhang Y, & Zhou X. Rapid visual detection of calcium ions using glutathione functionalized gold nanoparticles. *2011 Third International Conference of Measuring Technology and Mechatronics Automation (ICMTMA 2011)* **2011**; 2, 948–951. DOI: 10.1109/ICMTMA.2011.519

[27] Fu R, Li J, & Yang W. Aggregation of glutathione-functionalized Au nanoparticles induced by Ni2+ ions. *Journal of Nanoparticle Research* **2012**; 14(6), Art. No. 929. DOI: 10.1007/s11051-012-0929-y

[28] Feng B, Zhu R, Xu S, Chen Y, & Di J. A sensitive LSPR sensor based on glutathione-functionalized gold nanoparticles on a substrate for the detection of Pb2+ ions. *RSC Advances* **2018**; 8(8), 4049–4056. DOI: 10.1039/c7ra13127e

[29] Shi R, Liu XJ, & Ying Y. Glutathione-Capped Gold Nanoparticles-Based Photoacoustic Sensor for Label-Free Detection of Lead Ions. *Journal of Applied Spectroscopy* **2017**; 84(3), 401–406. DOI: 10.1007/s10812-017-0483-6

[30] Yu Y, Hong Y, Gao P, & Nazeeruddin MK. Glutathione Modified Gold Nanoparticles for Sensitive Colorimetric Detection of Pb2+ Ions in Rainwater Polluted by Leaking Perovskite Solar Cells. *Analytical Chemistry* **2016**; 88(24), 12316–12322. DOI: 10.1021/acs.analchem.6b03515

[31] Chai F, Wang C, Wang T, Li L, & Su Z. Colorimetric detection of Pb2+ using glutathione functionalized gold nanoparticles. *ACS Applied Materials and Interfaces* **2010**; 2(5), 1466–1470. DOI: 10.1021/am100107k

[32] Briñas RP, Hu M, Qian L, Lymar ES, & Hainfeld JF. Gold nanoparticle size controlled by polymeric Au(I) thiolate precursor size. *Journal of the American Chemical Society* **2008**; 130(3), 975–982. DOI: 10.1021/ja076333e

[33] Leverrier P, Montigny C, Garrigos M, & Champeil P. Metal binding to ligands: Cadmium complexes with glutathione revisited. *Analytical Biochemistry* **2007**; 371(2), 215–228. DOI: 10.1016/j.ab.2007.07.015

[34] Po³eæ-Pawlak K, Ruzik R, & Lipiec E. Investigation of Cd(II), Pb(II) and Cu(I) complexation by glutathione and its component amino acids by ESI-MS and size exclusion chromatography coupled to ICP-MS and ESI-MS. *Talanta* **2007**; 72(4), 1564–1572. DOI: 10.1016/j.talanta.2007.02.008

[35] Guan J, Jiang L, Zhao L, Li J, & Yang W. pH-dependent response of citrate capped Au nanoparticle to Pb2+ ion. *Colloids Surfaces A: Physicochemical and Engineering Aspects* **2008**; 325(3), 194–197. DOI: 10.1016/j.colsurfa.2008.05.003